pISSN 1229-3008 eISSN 2287-6251
Progress in Superconductivity and Cryogenics
Vol.18, No.2, (2016), pp.1~4 http://dx.doi.org/10.9714/psac.2016.18.2.001

Local transport properties of coated conductors by laser-scan imaging methods

Gracia Kim[a], William Jo[b,*], Dahyun Nam[c], Hyeonsik Cheong[c], and Seoung Hyun Moon[d]

[a] *Spin Engineering Physics Team, Korea Basic Science Institute (KBSI), Daejeon, Korea*
[b] *Department of Physics, Ewha Womans University, Seoul, Korea*
[c] *Department of Physics, Sogang University, Seoul, Korea*
[d] *SuNAM Co., Ltd, Gyonggi-do, Korea*

(Received 2 June 2016; revised or reviewed 23 June 2016; accepted 24 June 2016)

Abstract

To observe the superconducting current and structural properties of high critical temperature (T_c) superconductors (HTS), we suggest the following imaging methods: Room temperature imaging (RTI) through thermal heating, low-temperature bolometric microscopy (LTBM) and Raman scattering imaging. RTI and LTBM images visualize thermal-electric voltages as different thermal gradients at room temperature (RT) and superconducting current dissipation at near-T_c, respectively. Using RTI, we can obtain structural information about the surface uniformity and positions of impurities. LTBM images show the flux flow in two dimensions as a function of the local critical currents. Raman imaging is transformed from Raman survey spectra in particular areas, and the Raman vibration modes can be combined. Raman imaging can quantify the vibration modes of the areas. Therefore, we demonstrate the spatial transport properties of superconducting materials by combining the results. In addition, this enables visualization of the effect of current flow on the distribution of impurities in a uniform superconducting crystalline material. These imaging methods facilitate direct examination of the local properties of superconducting materials and wires.

Keywords : Room temperature imaging through thermal heating, low-temperature bolometric microscopy, Raman scattering spectroscopy

1. INTRODUCTION

Several groups have reported improvement of the properties of high T_c superconductors (HTS) for power applications [1, 2]. However, the development of HTS—especially REBCO (RE=rare earth) coated conductors (CCs)—is subject to critical fundamental material issues, such as disoriented grains, cation disorder, oxygen vacancy, and secondary phases [3-5], which influence the superconducting properties. Therefore, methods of quality monitoring of CCs have been investigated to develop a large-scale and a high production rate process. The existing *in-situ* quality control methods are complex in terms of both measurement and preparation. We suggest effective laser scanning-based imaging methods for investigating the local issues and surface morphology of HTS. The laser-based methods can be applied at both a normal state at RT and superconducting state at LT, facilitating simple and non-destructive measurements of superconducting materials. In this paper, we introduce three methods: Room temperature imaging (RTI) through thermal heating, low-temperature bolometric microscopy (LTBM), and Raman scattering imaging. These enable direct visualization of local issues with a 1-2 μm spatial resolution.

***** Corresponding author: wmjo@ewha.ac.kr

2. EXPERIMENTAL DETAILS

The RTI method involves measurement of thermal-electric voltages as different thermal gradients with different Seebeck coefficients between adjacent spots. The surface is scanned with a heating source: a 632 nm wavelength (λ) He-Ne laser. The Seebeck coefficients are related to the components and crystal orientation. In the case of YBCO in the superconducting state (90 K), the Seebeck coefficients of the *c*-axis and *ab*-plane are S_c: 2.3 μV/K and S_{ab}: 2.5 μV/K, respectively [6]. As a quality control method, the RTI method evaluates the surface grain structures. The grain structures of CCs must be clarified, because the current-carrying capacity of superconductors is linked to the local microstructure. The images provide morphological information, such as grain boundaries, grain sizes, and positions of impurities. This method has been used to evaluate the quality of solar cells and semiconducting devices [7-10].

LTBM is a unique imaging method for superconductors that enable characterization of the superconducting current. The measurement is operated on superconducting state as apply a suitable bias current (I_b). The local current transport properties as a function of the position are measured using a He-Ne laser as the heating source. RTI and LTBM can be performed in a similar way using the same chamber simultaneously. It is possible to obtain the bolometric

response of the superconducting transition, and to carry out structural fails on the superconducting matrix. The flux flow voltage in the images indicates either 1) the vicinity of defects or 2) weak superconducting area. Because the superconducting current circumvents the defects, so the areas where around defects have relatively higher the current density then the other areas. Also, weak areas have poor superconducting properties, meaning that the superconducting state at the spots can be changes to the normal state by local heating. The LTBM measurement parameters are changed every time, because liquid nitrogen (LN2) is hard to make a stable despite use of nitrogen gas to maintain the pressure. (2) LTBM images are obtained at a sufficiently low temperature. The film is not burned even if the temperature of the chamber increases suddenly increased. In addition, if an unsuitable I_b is applied, the current carrying capacity will reach the limit at the weak spots. Therefore, all LTBM parameters depend on different the condition and the materials. The details and principle of the technique are explained elsewhere [11].

Raman scattering spectroscopy can reveal quantitative compositions. Raman spectroscopy provides information on the materials, such as symmetry and phonon modes, oxygen concentrations, disorder, and secondary crystalline phases. Micro-Raman imaging is different from the other measurement techniques; it measures the Raman survey spectrum in a designated area with constant steps, and then integrates the area of a chosen mode as the function of the position. For low-intensity Raman modes, sometimes it is difficult to distinguish the signal from the fluctuations in the background signal. Therefore, one should use caution when analyzing Raman images of low-intensity modes.

3. RESULTS

We used two commotional $GdBa_2Cu_3O_{7-y}$ (GdBCO) coated conductors with different critical currents (I_c). GdBCO-coated conductors were fabricated on IBAD-MgO templates by ultrafast reactive co-evaporation: deposition and reaction (RCE-DR) process by SuNAM Co., Ltd. Experimental details and properties of the CCs are described elsewhere [12].

To evaluate the structural properties, we measured RIT images. Figure 1 shows response voltage and phase images of GdBCO. Before imaging, we fabricated a micro-bridge using photolithography and chemical wet-etching processes. The micro-bridge surface had an area of 150 μm × 1000 μm; however, its actual size was 172 μm × 1030 μm due to over etching. We observe the surface structure of solidified flux as fast conversion from liquid phases to on Gd123 phases [12]. In addition, the size of the granules on the surface and the intensity can be estimated from the voltage signal. The phase image shows changing the degrees at the broader between the impurities and uniform areas as different the sign of the thermal voltages. The voltages are related to the difference in the Seebeck

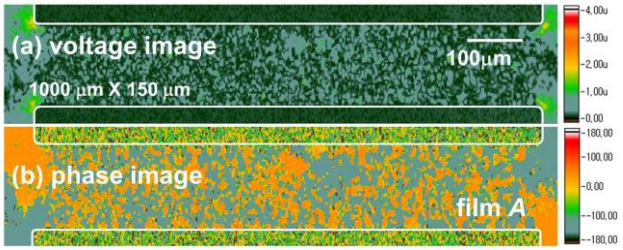

Fig. 1. RTI of GdBCO film *A*. The scale bar is inset into the images. The unit for (a) voltage and (b) phase image are μV and degrees, respectively.

coefficients due to the tilted crystalline, defects and oxygen concentration. Although the images are similar to existed optical imaging methods however we also obtain the location of invisible impurities as difference Seebeck coefficients.

Figure 2 displays LTBM images and micro-Raman scattering spectra of a GdBCO film *A*. Figure 2 (a) shows bias current-dependent LTBM images at 91.1 K with I_b values of 250 and 280 mA, respectively. The border of the micro-bridge and the scale bars are denoted in the images by dotted and bold lines, respectively. As the I_b increases, the flux flow appears with the shape of rounds successively. The increasing response voltage is due to the increased flow due to interruption of superconducting current. In other words, the defects block the current path, a bottleneck effect. The current flow mechanism is not different between short and long samples. However, the equipment has a limitation to measure the long sample. So, we have tried to apply the bolometric methods as an *in-situ* monitoring system in the fabrication processes of CCs through the scale-up.

SmBCO and GdBCO-coated conductors show defects of different shapes [13]. LTBM images of SmBCO CC show line defects, indicating that the CC has uniformity, at least in the width direction. The SmBCO films were fabricated by a double-step process, and both the depositions and the partial oxygen treatments were repeated more than 1000 times during the process. This indicates that the fabricated film is flatter and steadier than that produced using the single-path fabrication process [14]. However, the GdBCO films were produced using a RCE-DR process, which has a single path on the stability diagram [12]. From the difference the shape of defects in LTBM images, we suppose that the different processes might be affected to develop different kind of defects.

We performed micro-Raman scattering spectroscopy to confirm the compositions of two areas in the LTBM image. In Figure 2(b), the black and red lines represent the normal surface and several impurity phases respectively. The micro-Raman scattering spectra of the selected areas were measured using 200 seconds acquisition. Raman acquisition time decides the ratio of signal to noise. If the acquisition time is longer, the noise would be reduced. However, there is a risk to damage on the film surface as

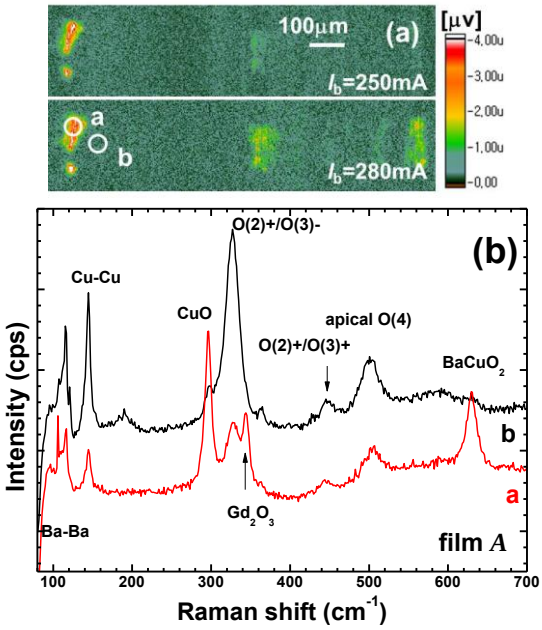

Fig. 2. LTBM (upper) and micro-Raman scattering spectra (bottom) of GdBCO film *A*. The LTBM image was measured at 91.1 K with 250 mA and 280 mA of I_b, respectively.

increasing the acquisition time. The black spectrum is similar to a previous report of polarized Raman scattering spectroscopy of SmBCO coated conductors [13]. This indicates that the normal surface of GdBCO has well-aligned orthorhombic compounds [15]. The changes between the two spectra are the intensities of an out-of-phase mode (O(2)+/O(3)-) and the secondary phases. The out-of-phase mode is linked to the *c*-axis orientation, meaning that its intensity should be maximum in well-aligned REBCO compounds. The red line has not only major orthorhombic REBCO peaks [13], very different from the black line, but also secondary phases such as CuO, Gd_2O_3 and $BaCuO_2$. In addition, the intensity of out-of-phase modes differs by more than 10% between the high- and low-voltage regions. This indicates that the high-voltage regions consist of REBCO compounds and the secondary phases.

In the same way, we measured LTBM images of GdBCO film *B* at 90.8 K with ±50 mK of temperature range, as shown in Figure 3. In Figure 3(a), despite the line noise, dissipation voltage areas appear due to interruption of the current flow at I_b = 340 mA. The high-voltage regions, indicated by two small circles, are evident on the right side of the micro-bridge. In Figure 2(a), the defects are randomly spread and are of a round shape. To analyze the components, we chose a square area consisting of high- and low-voltage regions to evaluate the current-limiting phenomena at the micro-scale.

The Raman images are constructed using three different modes from the survey spectra. From the left, each image shows (b) an out-of-phase mode, (c) the ratio in-/out-of-phase modes and (d) the secondary phase: $BaCuO_2$ mode, respectively. These modes should be selected in survey spectra for the following reasons: (1) the out-of-phase mode (O(2)+/O(3)-) is highly dependent on the *c*-axis orientation. So, the film is grown with a *c*-axis orientation, and the peak area is larger and sharper. Thus the peak shows high intensity, and the film can carry the superconducting current flow without loss. (2) The intensity of in-phase modes (O(2)+/O(3)+) is linked to the *a*-axis orientation. So, it should be negligible in a well-grown film. As mentioned above, Raman imaging involves conversion of the peak area from the survey spectrum of each spot. Therefore, the images enable quantitation of each component, and the brightness is proportional to the concentration. So, the signal intensity will be opposite that of the out-of-phase modes. (3) A $BaCuO_2$ secondary-phase mode is randomly observed in the film surface, as confirmed by XRD. Also, this peak does not overlap with the other peaks; therefore, the area can be calculated using integration.

Figure 3(b) shows the out-of-phase modes. The bottom side of images has higher intensity than the top side, meaning that the bottom side has a superior *c*-axis orientation than the top side. In Figure 3(c), the in-/out-of-phase mode ratio has contrasting colors to that in Figure 3(b). This result is consistent with the LTBM image. In addition, Figure 3(d) shows the intensity of the $BaCuO_2$ secondary phase mode, which corresponds to the regions of high intensity of Figure 3(c).

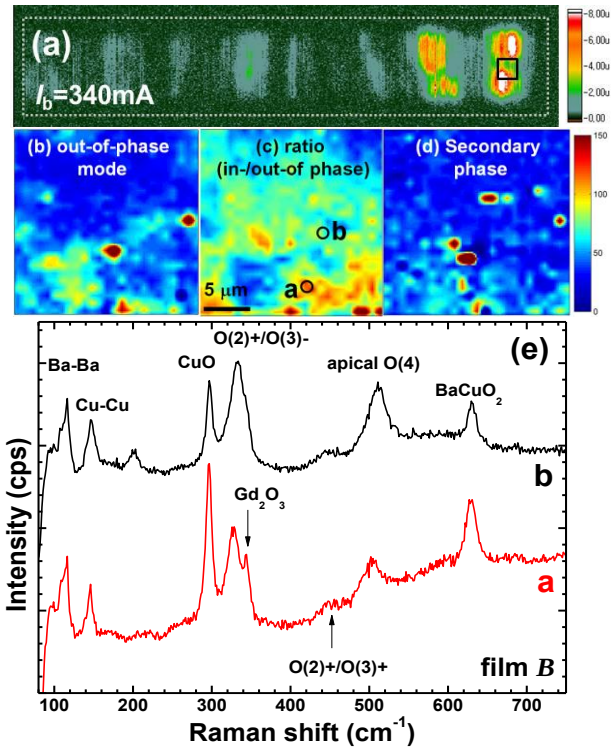

Fig. 3. (a) LTBM images with 340 mA of I_b (top), Raman images (middle): (b) out-of phase mode, (c) ratio of in-/out-of phase mode and (d) $BaCuO_2$ mode (e) Micro-Raman scattering spectra of GdBCO film *B* (bottom).

Therefore, it can be demonstrated that the high-voltage response regions in LTBM image has a large amount of *a*-axis orientation and some secondary phases. In addition, we performed micro-Raman scattering spectroscopy to confirm the accuracy of Raman imaging. Figure 3(e) shows the micro-Raman spectrum, of film *B*, obtained at a high (red) and low (black) intensity, respectively. The survey spectrum (black-bold line) is similar to the macro-polarized Raman scattering spectrum, as reported previously [13, 16]. In contrast, we observe the high intensity of secondary phases in red line. The peaks at 145 and 500 cm^{-1} are ascribed to Cu-Cu stretching in the CuO_2 plane and apical O(4) phonon band modes along the *c*-axis, respectively. In addition, the Ba-Ba stretching bending modes in the CuO_2 plane near 100 cm^{-1} consist of multiple peaks of different frequencies due to the presence of different Ba-Ba phases in the film. In addition, the O(4) mode is shifted in the low frequency direction in the red spectrum, because it is highly sensitive to oxygen vacancies. In summary, we confirm that the low- and high-voltage regions on the film surface have different phases, the axis and concentration of the secondary phases. The Raman images are in agreement with LTBM images, indicating that the high response-voltage regions in LTBM images are related to inhomogeneity 123 phases. The results suggest that these imaging methods are useful for analysis of localized structural properties [17].

4. CONCLUSION

In this paper, we report imaging methods of the structural and electrical properties of superconducting wires and materials. The RIT and LTBM are specialized methods for evaluation of the surface morphology and spatial distribution respectively of superconductors at a micro-scale. Raman scattering spectroscopy enables quantitation of components on a specific area of the surface. And also, Raman imaging can compose the several vibration modes. It means the methods easily intelligible to the distribution of each component of the materials. We performed RIT and LTBM to investigate the spatial distribution of structural properties at RT and flux flow voltages below the T_c, respectively. RIT and bias current-dependent LTBM images show the uniform areas and current distribution on the surface. In micro-Raman scattering spectroscopy, the high-voltage regions in LTBM images are linked to some secondary phases. The current distribution in LTBM showed a good correlation between the positions of defects. The imaging methods being in this study enable the quality monitoring to improve the performance of superconducting materials and wires.

ACKNOWLEDGMENTS

This work was supported by National Research Foundation (NRF) grants funded by the Korean government (MSIP) (No. NRF-2014R1A2A2A01004070) and (No. 2015001948).

REFERENCES

[1] Y. Shiohara, M. Yoshizumi, T. Izumi and Y. Yamada, "Present status and future prospect of coated conductor development and its application in Japan," *Supercond. Sci. Technol.*, vol. 21, pp. 1-7, 2008.

[2] M. Chen, L. Donzel, M. Lakner and W. Paul, "High temperature superconductors for power applications," *J. Eur. Ceram. Soc.*, vol. 24, pp. 1815, 2004.

[3] K. Salama, S. P. Athur and U. Balachandran, "Texturing of REBCO using temperature gradient," *Physica C*, vol. 357-360, pp. 11-19 2001.

[4] T. Aytug, M. Paranthaman, L. Heatherly, Y. Zuev, Y. Zhang, K. Kim, A. Goyal, V. A. Maroni, Y. Chen and V. Selvamanickam, "Deposition studies and coordinated characterization of MOCVD YBCO films on IBAD-MgO templates," *Supercond. Sci. Technol.*, vol. 22, pp. 015008, 2006.

[5] E. Goodilin, M. Limonov, A. Panfilov, N. Khasanova, A. Oka, S. Tajima and Y. Shiohara, "Oxygen nonstoichiometry and phase transitions of the neodymium-rich $Nd_{1+x}Ba_{2-x}Cu_3O_z$ solid solution," *Physica C*, vol. 300, pp. 250, 1998.

[6] C. Hohn, M. Galffy, A. Dascoulidou, A. Freimuth, H. Soltner and U. Poppe, "Seebeck-effect in the mixed state of Y-Ba-Cu-O," *Z. Phys. B - Condensed Matter*, vol. 85, pp. 161-168, 1991.

[7] J. A. Walraven, Edward I. Cole Jr. and P. Tangyunyong, "Failure Analysis of MEMS Using Thermally-Induced Voltage Alteration," *International Symposium for Testing and Failure Analysis*, 2000.

[8] D. A. Redfern, J. A. Thomas, C. A. Musca, J. M. Dell and L. Faraone, "Diffusion length measurements in p-HgCdTe using laser beam induced current," *J. Electron. Mater.*, vol. 30, pp. 696, 2001.

[9] S. A. Galloway, P. R. Edwards and K. Durose, "Characterization of thin-film CdS/CdTe solar cells using electron beam induced current," *Solar Energy Materials & Solar Cells*, vol. 57, pp. 61-74, 1999.

[10] E. I. Cole Jr., P. Tangyunyong, D. A. Benson and D. L. Barton, "TIVA and SEI development for Enhanced Frond and Backside Interconnection Failure Analysis," *Microelectronics Reliability*, vol. 39, pp. 991-996, 1999.

[11] G. Kim, W. Jo, A. Matsekh, M. Inoue, T. Kiss, H.-S. Ha and S. S. Oh, "Current Limiting Phenomena in $SmBa_2Cu_3O_7$ Coated Conductors Observed by Laser-Induced Thermoelectric Imaging and Low-Temperature Laser Scanning Microscopy," *IEEE Trans. Appl. Supercon.*, vol. 21, pp. 3421, 2011.

[12] J. L. MacManus-Driscoll, M. Bianchetti, A. Kursumovic, G. Kim, W. Jo, H. Wang, J. H. Lee, G. W. Hong and S. H. Moon, "Strong pinning in very fast grown reactive co-evaporated $GdBa_2Cu_3O_7$ coated conductors," *APL Materials*, vol. 2, pp. 086103, 2014.

[13] G. Kim, H. J. Jin, W. Jo, D. H. Nam, H. Cheong, H.S. Kim, S.S. Oh, R.K. Ko, Y.S. Jo and D.W. Ha, "Ultra-large current transport in thick $SmBa_2Cu_3O_{7-x}$ films grown by reactive co-evaporation," *Physica C*, vol. 513, pp. 29–34, 2015.

[14] H. S. Kim, S.-S. Oh, H.-S. Ha, D. Youm, S.H. Moon, J. H. Kim, S. X. Dou, Y.U. Heo, S. H. Wee and A. Goyal, "Ultra-High Performance, High-Temperature Superconducting Wires via Cost-effective, Scalable, Co-evaporation Process," *Sci. Rep.*, vol. 4, pp. 4744, 2014.

[15] K. Venkataraman, R. Baurceanu and V. A. Maroni, "Characterization of $MBa_2Cu_3O_{7-x}$ Thin Films by Raman Microspectroscopy," *Applied Spectroscopy*, vol. 59, pp. 639, 2005.

[16] G. Kim, W. Jo, H.-S. Ha, S. S Oh, D. Y. Park and H. Cheong, "Characterization of Co-Evaporated $SmBa_2Cu_3O_7$ Coated Conductors by Polarized-Raman Scattering Spectroscopy," *IEEE Trans. Appl. Supercon.*, vol. 21, pp. 3352, 2011.

[17] G. Kim, H.-J. Jin and W. Jo, "Optical imaging methods for qualification of superconducting wires," *Progress in Superconductivity and Cryogenics*, vol. 16, pp. 21-24, 2014.